7

Synchronization phenomena in networks

Many natural systems can be described as a collection of oscillators coupled to each other via an interaction matrix. Systems of this type describe phenomena as diverse as earthquakes, ecosystems, neurons, cardiac pacemaker cells, or animal and insect behavior. Coupled oscillators may display synchronized behavior, i.e. follow a common dynamical evolution. Famous examples include the synchronization of circadian rhythms and night/day alternation, crickets that chirp in unison, or flashing fireflies. An exhaustive list of examples and a detailed exposition of the synchronization behavior of periodic systems can be found in the book by Blekhman (1988) and the more recent reviews by Pikovsky, Rosenblum and Kurths (2001), and Boccaletti *et al.* (2002).

Synchronization properties are also dependent on the coupling pattern among the oscillators which is conveniently represented as an interaction network characterizing each system. Networks therefore assume a major role in the study of synchronization phenomena and, in this chapter, we intend to provide an overview of results addressing the effect of their structure and complexity on the behavior of the most widely used classes of models.

7.1 General framework

The central question in the study of coupled oscillators concerns the emergence of coherent behavior in which the elements of the system follow the same dynamical pattern, i.e. are synchronized. The first studies were concerned with the synchronization of periodic systems such as clocks or flashing fireflies. More recently, much interest has also been devoted to the possible synchronization of chaotic systems (see Boccaletti *et al*. [2002] for a recent review), whose existence can seem paradoxical but occurs in systems as diverse as lasers (Otsuka *et al*., 2000) or neural networks (Hansel and Sompolinsky, 1992), and is very relevant in many physiological processes (Glass, 2001). Chaotic systems are characterized by a very strong

https://doi.org/10.1017/CBO9780511791383.008 Published online by Cambridge University Press

sensitivity to initial conditions, and two identical chaotic systems will become uncorrelated at large times even if they start from very similar (but not identical) states. Nevertheless, the coupling of such systems can lead them to follow the same chaotic trajectories in the available phase space.

In order to frame precisely how the network structure enters the problem of synchronization, let us consider a large number N of oscillators (units) in interaction. Each oscillator i is described by an internal degree of freedom $\phi_i(t)$ $(i = 1, \ldots, N)$ which evolves in time both because of an internal dynamics and because of the coupling with the other units. A quite general form to describe the evolution of the system is given by the set of equations

$$\frac{\mathrm{d}\phi_i}{\mathrm{d}t} = f_i(\{\phi\}), \tag{7.1}$$

where $\{\phi\}$ represents the set of all ϕ_i's. Each unit, if isolated, can reach at large times either a stable fixed point, a limit cycle, or a chaotic strange attractor (Bergé, Pomeau and Vidal, 1984). The set of units and their evolution equations (7.1) can be seen as a network in which each node represents an oscillator and two nodes i and j are linked by a directed edge from j to i if the evolution equation of i depends on the state ϕ_j of oscillator j. While this definition leads to the emergence of a directed network, the case of symmetric interactions is most often considered: the evolution of ϕ_j depends on ϕ_i and vice versa, so that the resulting network is undirected.

When a large number of units is coupled through a complex network of interactions, various types of synchronization behaviors are (a priori) possible. The equality of all internal variables (which evolve in time) $\{\phi_i(t) = s(t), \forall i\}$ is called *complete synchronization* and is the most commonly studied synchronization phenomenon (Pecora and Carroll, 1990). *Phase synchronization* (Rosenblum, Pikovsky and Kurths, 1996) is a weaker form of synchronization which can be reached by oscillators described by a phase and an amplitude: it consists in a locking of the phases while the correlation between amplitudes is weak. *Generalized synchronization* of two dynamical units is an extension of the synchronization concept in which the output of one unit is constantly equal to a certain function of the output of the other unit (Rulkov *et al.*, 1995).[1] More complex phenomena such as intermittent bursts of non-synchronized behaviors in between periods of synchronized evolution can also be observed. Most studies have, however, focused on the case of complete synchronization (see Boccaletti *et al.* [2006] for a recent review), and we will limit our presentation to this case in the present chapter.

[1] The generalized synchronization is therefore an involved phenomenon which may not easily be detected by the simple observation of the evolution of the dynamical variables $\{\phi\}$.

https://doi.org/10.1017/CBO9780511791383.008 Published online by Cambridge University Press

In general, the synchronization behavior is the result of a combination of the connectivity pattern and the specific oscillators and interaction functions. The remaining sections of this chapter are therefore devoted to specific models or classes of models as identified by the properties of each oscillator and their interaction function.

7.2 Linearly coupled identical oscillators

Given a system of coupled oscillators, the issue of the existence and stability of a synchronized state can be tackled analytically by assuming a specific form for the oscillators' interactions. The first model that is natural to consider is a collection of N identical dynamical units, each of them endowed with an internal degree of freedom ϕ_i (for simplicity we consider scalar ϕ_i, but the discussion can easily be extended to the vectorial case). Each unit, if isolated, evolves according to an identical internal dynamics governed by a local ordinary differential equation of the form

$$\frac{\mathrm{d}\phi_i}{\mathrm{d}t} = F(\phi_i)\,,\ i = 1, \ldots, N. \tag{7.2}$$

When the units are interconnected through an interaction network, the previous equation is modified since each unit i interacts with its neighbors $j \in \mathcal{V}(i)$. A simple example corresponds to the *linear* coupling, for which each unit i is coupled to a linear superposition of the outputs of the neighboring units, and for which the evolution equations of the system take the form

$$\frac{\mathrm{d}\phi_i}{\mathrm{d}t} = F(\phi_i) + \sigma \sum_{j=1}^{N} C_{ij} H(\phi_j). \tag{7.3}$$

Here H is a fixed output function, σ represents the interaction strength, and C_{ij} is the *coupling matrix*. In this section, we restrict the discussion to identical oscillators and output functions (same functions F and H for all units). One can moreover assume that the coupling between two units depends only on the difference between their outputs. In this case, each node i evolves according to both its internal dynamics and the sum of the differences between its output function and the ones of its neighbors as

$$\frac{\mathrm{d}\phi_i}{\mathrm{d}t} = F(\phi_i) + \sigma \sum_{j \in \mathcal{V}(i)} \left[H(\phi_i) - H(\phi_j) \right]. \tag{7.4}$$

This corresponds to the coupling $C_{ij} = L_{ij}$ where L_{ij} is the Laplacian matrix of the interaction network. As recalled in Appendix 4, $L_{ij} = -1$ for $i \neq j$ if and only if i and j are connected by a link (otherwise $L_{ij} = 0$), and L_{ii} is the degree of node i, i.e. the number of units to which i is connected.

https://doi.org/10.1017/CBO9780511791383.008 Published online by Cambridge University Press

The functions F and H and the structure of the evolution equations are crucial for the subsequent analysis and the existence of a fully synchronized solution of the evolution equations. Let us denote by $s(t)$ the evolution of the uncoupled oscillators, according to Equation (7.2). It is then straightforward to see that the fully synchronized behavior $\{\phi_i(t) = s(t),\ \forall i\}$ is also a solution of (7.4). The stability of this synchronized state can be studied by using the *master stability function* approach that considers a small perturbation $\phi_i = s + \xi_i$ of the system, with $\xi_i \ll s$, close to the synchronized state.[2] The synchronized state is then *stable* if and only if the dynamical evolution drives the system back to a synchronized state by a steady decrease of the perturbation ξ_i. If the perturbation increases the synchronized state is unstable. In order to distinguish between these two cases, we have to determine the evolution equation of the perturbation. To this aim, we can expand the quantities appearing in the evolution equation of ϕ_i as $F(\phi_i) \approx F(s) + \xi_i F'(s)$ and $H(\phi_j) \approx H(s) + \xi_j H'(s)$, where F' and H' denote the derivatives of the functions F and H with respect to s. Since $s(t)$ is by definition solution of $ds/dt = F(s(t))$, the evolution equation for the perturbations $\xi_i(t)$ can be written as

$$\frac{\mathrm{d}\xi_i}{\mathrm{d}t} = F'(s)\xi_i + \sigma \sum_j \left[L_{ij} H'(s)\right] \xi_j. \tag{7.5}$$

The symmetry of the Laplacian matrix L implies that its N eigenvalues, λ_i ($i = 1, \ldots, N$) are real and non-negative. The fact that $\sum_j L_{ij} = 0$ ensures that one of these eigenvalues is null, we can therefore order them as $0 = \lambda_1 \leq \lambda_2 \leq \cdots \leq \lambda_N \equiv \lambda_{\max}$. The system of equations can be decoupled by using the set of eigenvectors ζ_i which are an appropriate set of linear combinations of the perturbations ξ_j, obtaining

$$\frac{\mathrm{d}\zeta_i}{\mathrm{d}t} = \left[F'(s) + \sigma\lambda_i H'(s)\right] \zeta_i. \tag{7.6}$$

At short times, one can assume that s almost does not vary, and these decoupled equations are easily solved, with the solutions

$$\zeta_i(t) = \zeta_i^0 \exp\left\{[F'(s) + \sigma\lambda_i H'(s)]t\right\}, \tag{7.7}$$

where ζ_i^0 is the initially imposed perturbation. These equations show that the perturbation will either increase or decrease exponentially, depending on the signs of the quantities $\Lambda_i \equiv F'(s) + \sigma\lambda_i H'(s)$. The eigenvalue $\lambda_1 = 0$ gives $\Lambda_1 = F'(s)$ and is only related to the evolution of each single unit, which is either chaotic (if

[2] We present here the case in which the units obey continuous time evolutions, but the case of time-discrete maps can be analyzed along similar lines; see Jost and Joy (2001), Jalan and Amritkar (2002), Lind, Gallas and Herrmann (2004).

https://doi.org/10.1017/CBO9780511791383.008 Published online by Cambridge University Press

$F'(s) > 0$) or periodic. For the synchronized state to be stable, *all* the other components of the perturbation ζ_i have to decrease, which means that all the Λ_i, for $i = 2, \ldots, N$, need to be negative. This has to be true for all values of s taken by the system during its synchronized evolution. The master stability function is thus defined as (Heagy, Pecora and Carroll, 1995; Pecora and Carroll, 1998; Barahona and Pecora, 2002)

$$\Lambda(\alpha) = \max_s \left(F'(s) + \alpha H'(s) \right), \tag{7.8}$$

where the max is taken over the trajectory defined by $\mathrm{d}s/\mathrm{d}t = F(s(t))$,[3] and the stability condition of the synchronized state translates into the condition that all $\sigma\lambda_i$, for $i = 2, \ldots, N$, are located in the negative region of the master stability function, i.e. are such that $\Lambda(\sigma\lambda_i) \leq 0$. For $\alpha > 0$, various cases can be distinguished: if $\Lambda(\alpha)$ is always positive, the synchronized state is never stable. If $\Lambda(\alpha)$ decreases and becomes negative for all $\alpha > \alpha_c$, it is on the other hand enough to have a large enough coupling strength ($\sigma > \alpha_c/\lambda_2$) to ensure synchronization.

A more interesting situation, which corresponds to a large class of functions F and H (Barahona and Pecora, 2002) is sketched in Figure 7.1. In this case $\Lambda(\alpha)$ takes negative values for α between α_1 and α_2 and the necessary condition for stability of the synchronous state is then $\sigma\lambda_i \in [\alpha_1, \alpha_2]$ for $i = 2, \ldots, N$. This criterion is not straightforward: it seems indeed quite natural that the coupling σ should be large enough, which explains the lower bound $\sigma\lambda_2 \geq \alpha_1$, but on the other hand it cannot be increased indefinitely as it might cause destabilization of

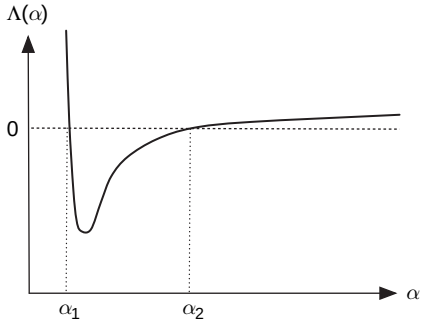

Fig. 7.1. Typical master stability function. The synchronized state is stable only if all the positive eigenvalues λ_i of the Laplacian are such that $\Lambda(\sigma\lambda_i) \leq 0$, which corresponds to $\sigma\lambda_i \in [\alpha_1, \alpha_2]$ for $i = 2, \ldots, N$. Adapted from Barahona and Pecora (2002).

[3] If the variables ϕ_i are d-dimensional vectors, then the ζ_i are also vectors, $F'(s)$ and $H'(s)$ are $d \times d$ matrices, and $\Lambda(\alpha)$ is the maximal eigenvalue of the matrix $F'(s) + \alpha H'(s)$.

the synchronous state when $\sigma\lambda_{\max}$ becomes larger than α_2. The condition for synchronization is then satisfied if the coupling σ lies between α_1/λ_2 and $\alpha_2/\lambda_{\max}$ and a compact way to express if the network is synchronizable (Barahona and Pecora, 2002) reads as

$$\frac{\lambda_{\max}}{\lambda_2} < \frac{\alpha_2}{\alpha_1}, \tag{7.9}$$

where λ_2 and $\lambda_{\max}$ are the first non-zero and maximum eigenvalues of the Laplacian matrix, respectively. The condition (7.9) is particularly interesting since it separates the spectral properties of the network, which determine the *eigenratio* $\lambda_{\max}/\lambda_2$, from the properties of the oscillators (F and H), which govern α_2 and α_1. Strikingly, for given functions F and H, some networks will have too large a value of $\lambda_{\max}/\lambda_2$ and therefore cannot exhibit synchronized behavior, whatever the value of the coupling parameter σ.

The previous result clearly shows the role of the interaction pattern in synchronization phenomena and has led to the study of the general propension towards synchronization of different network topologies, *independently of the nature of the oscillators*. Networks with smaller eigenratio $\lambda_{\max}/\lambda_2$ will indeed favor synchronization of whichever oscillators they couple. The synchronizability of different networks is therefore obtained by investigating the eigenvalues of the corresponding coupling matrices $\mathbf{C}$. Various studies have been devoted to this problem and in the following sections we will see how the eigenratio $\lambda_{\max}/\lambda_2$ varies according to the properties of networks, and which kinds of networks can minimize it.

7.2.1 Small-world networks

As mentioned in the previous chapter, one of the motivations behind the formulation of the Watts–Strogatz model (Watts and Strogatz, 1998) was the investigation of the synchronization properties of real-world networks and how clustering might favor synchronizability (Gade and Hu, 2000; Lago-Fernández *et al.*, 2000). In the case of identical oscillators with linear coupling, Barahona and Pecora (2002) have provided a thorough comparison of the synchronizability of small-world systems. At first they analyzed the two limiting cases of a random Erdős–Rényi graph and a one-dimensional ordered ring. For a ring of N nodes, each coupled to its $2m$ nearest neighbors, the eigenvalues $\lambda_{\max}$ and λ_2 of the Laplacian matrix are given by $\lambda_{\max} \sim (2m+1)(1+2/3\pi)$ for $m \gg 1$, and $\lambda_2 \sim 2\pi^2 m(m+1)(2m+1)/(3N^2)$ for $m \ll N$, so that the eigenratio

$$\frac{\lambda_{\max}}{\lambda_2} \propto \frac{N^2}{m(m+1)} \tag{7.10}$$

https://doi.org/10.1017/CBO9780511791383.008 Published online by Cambridge University Press

increases rapidly with the number of oscillators at m fixed. For large N the synchronizability is less likely. This, however, improves by increasing m, and in the limit of a complete graph with $m = (N-1)/2$, the system always exhibits a synchronizability interval.

The Erdős–Rényi random graphs with connection probability p (average degree pN) represent the opposite limiting case. In this case the eigenratio can be explicitly written as (Mohar, 1997)

$$\frac{\lambda_{\max}^{\mathrm{ER}}}{\lambda_2^{\mathrm{ER}}} \simeq \frac{Np + \sqrt{2p(1-p)N\log N}}{Np - \sqrt{2p(1-p)N\log N}}. \tag{7.11}$$

The Erdős–Rényi random graph thus becomes synchronizable, in the sense that $\lambda_{\max}^{\mathrm{ER}}/\lambda_2^{\mathrm{ER}}$ becomes finite, for p larger than $2\log N/N$. This is close to the threshold value $\log N/N$ at which the Erdős–Rényi becomes "almost surely" connected. It is important to note that a random graph consisting of several disconnected components is by definition not synchronizable, since the various components are not able to communicate.

In order to interpolate between the ordered ring structure and the completely random Erdős–Rényi graph, Barahona and Pecora (2002) have altered the ordered ring by adding to each node additional edges randomly wired in the ring. In this way small-world networks with different values of the connectance $\mathcal{D} = 2E/(N(N-1))$ are obtained. The synchronizability of networks can be visually inspected in Figure 7.2 by comparing the behavior of the eigenratio

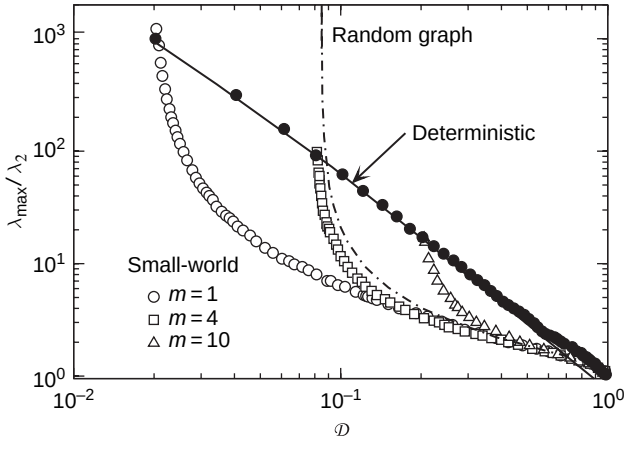

Fig. 7.2. Evolution of the eigenratio $\lambda_{\max}/\lambda_2$ as the connectance $\mathcal{D}$ is varied, for deterministic ring structures (black filled circles), small-world networks with various m (open symbols), and for the Erdős–Rényi random graph (dot-dashed line). The continuous line corresponds to Equation (7.10). Data from Barahona and Pecora (2002) with $N = 100$.

https://doi.org/10.1017/CBO9780511791383.008 Published online by Cambridge University Press

λ_{max}/λ_2 as a function of the graph connectance in the two limiting cases and for the small-world graphs. In general, an increasing connectance corresponds to an improvement in synchronizability. The small-world topology, however, exhibits better synchronizability properties than those found in ordered rings. Figure 7.2 provides evidence that the small-world topology is a viable route to improve synchronizability generally by only acting on the system connectivity pattern.

7.2.2 Degree fluctuations: the paradox of heterogeneity

While a naive generalization of the results of Barahona and Pecora (2002) could lead to the conclusion that networks get easier to synchronize when their diameter gets smaller, Nishikawa *et al.* (2003) have shown that the situation is not so simple. Small network diameters can be obtained by considering networks with power-law degree distribution $P(k) \sim k^{-\gamma}$ with decreasing γ. The surprising result of such a procedure is that the eigenratio λ_{max}/λ_2 of the Laplacian's largest and smallest non-zero eigenvalues *increases* strongly when γ decreases. In other words, as the network becomes more heterogeneous and shrinks in diameter, it becomes less synchronizable. The intuitive explanation of this effect lies in the "overloading" of the hubs by too many different inputs which come from the many oscillators to which they are connected (Nishikawa *et al.*, 2003). In general the inputs cancel each other if they have different phases or frequencies and hubs are not easily synchronizable. This effect is not a particular feature of the scale-free heterogeneity and is recovered in any network characterized by large hubs as shown by Nishikawa *et al.* (2003) on a variant of the Watts–Strogatz model. This variant of the model considers the basic small-world construction with N initial nodes forming a one-dimensional ring, each node having $2m$ connections to its nearest neighbors. In order to introduce a given number of hubs, n_c "centers" are chosen at random, and a fixed number of shortcuts are added between the n_c centers and nodes chosen at random. The level of heterogeneity is therefore tuned by n_c: smaller n_c leads to a large degree of the centers as well as to a small diameter of the network. The results obtained by Nishikawa *et al.* (2003) clearly show that this construction leads to large eigenratios λ_{max}/λ_2 and decreased synchronizability.

The fact that networks with heavy-tailed degree distributions and heterogeneous connectivity patterns are more difficult to synchronize than homogeneous networks has been dubbed the *paradox of heterogeneity* (Motter, Zhou and Kurths, 2005a; 2005b; 2005c). Interestingly, this evidence has led Motter *et al.* (2005a) to explore alternative ways to improve synchronizability in heterogeneous networks by relaxing the assumption of symmetric couplings between oscillators.

In particular, Motter *et al.* (2005a) have proposed the following coupling structure

$$\frac{\mathrm{d}\phi_i}{\mathrm{d}t} = F(\phi_i) + \frac{\sigma}{k_i^{\beta}} \sum_j L_{ij} H(\phi_j), \tag{7.12}$$

where L_{ij} is, as before, the Laplacian matrix, k_i is the degree of node i and β is a tunable parameter. The obtained coupling matrix $C_{ij} = L_{ij} k_i^{-\beta}$ is no longer symmetric. It can, however, be written as $C = D^{-\beta} L$, where $D = \mathrm{diag}\{k_1, \ldots, k_N\}$ is a diagonal matrix. The identity $\det(D^{-\beta} L - \lambda I) = \det(D^{-\beta/2} L D^{-\beta/2} - \lambda I)$, valid for any λ, shows that the eigenspectrum of C is the same as that of the symmetric matrix $D^{-\beta/2} L D^{-\beta/2}$, hence is real and non-negative.

The influence of β can be first understood through a mean-field approach (Motter *et al.*, 2005a). The evolution equation of ϕ_i, (7.12), can indeed be written as

$$\begin{aligned} \frac{\mathrm{d}\phi_i}{\mathrm{d}t} &= F(\phi_i) + \frac{\sigma}{k_i^{\beta}} \left[k_i H(\phi_i) - \sum_{j \in \mathcal{V}(i)} H(\phi_j) \right] \\ &= F(\phi_i) - \sigma k_i^{1-\beta} \left[\bar{H}_i - H(\phi_i) \right], \end{aligned} \tag{7.13}$$

where $\bar{H}_i \equiv \sum_{j \in \mathcal{V}(i)} H(\phi_j)/k_i$ is the average "field" of i's neighbors. If the network is sufficiently random, and if the system is close to the synchronized state s, $\bar{H}_i$ can be approximated by $H(s)$, so that one obtains the set of *decoupled* equations

$$\frac{\mathrm{d}\phi_i}{\mathrm{d}t} = F(\phi_i) - \sigma k_i^{1-\beta} \left[H(s) - H(\phi_i) \right], \tag{7.14}$$

and the condition for all oscillators to be synchronized by the common mean-field forcing $H(s)$ is that $\alpha_1 < \sigma k_i^{1-\beta} < \alpha_2$ for all i. For $\beta \neq 1$, it is then clear that as soon as one node has a degree different from the others, this condition will be more difficult to meet. On the other hand, $\beta = 1$ allows the network characteristics to be removed from the synchronizability condition. In the context of the above mean-field approximation the eigenratio reads as

$$\frac{\lambda_{\max}}{\lambda_2} = \begin{cases} \left(\frac{k_{\max}}{k_{\min}} \right)^{1-\beta} & \text{if } \beta \leq 1 \\ \left(\frac{k_{\min}}{k_{\max}} \right)^{1-\beta} & \text{if } \beta \geq 1 \end{cases}, \tag{7.15}$$

where $k_{\max}$ and $k_{\min}$ are respectively the maximum and minimum degree in the network. The minimum value for the eigenratio is therefore obtained for $\beta = 1$. The numerical computations of eigenvalue spectra confirm the mean-field result, and show a global minimum of $\lambda_{\max}/\lambda_2$ at $\beta = 1$ (see Figure 7.3). This minimum (almost) does not depend on the degree distribution exponent γ for various models of scale-free networks. Thanks to the compensation of the large degree of the hubs

https://doi.org/10.1017/CBO9780511791383.008 Published online by Cambridge University Press

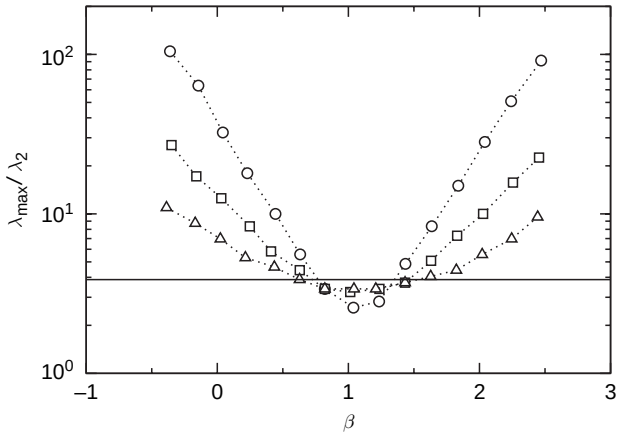

Fig. 7.3. Eigenratio λ_{max}/λ_2 as a function of β for random scale-free networks with $\gamma = 3$ (circles), $\gamma = 5$ (squares), $\gamma = 7$ (triangles), and $\gamma = \infty$ (line). Each symbol corresponds to an average over 50 different networks, with minimum degree 10 and size 1024. Data from Motter *et al.* (2005a).

by the $k_i^{-\beta}$ term, with $\beta = 1$, scale-free networks in fact become as synchronizable as random homogeneous networks. This effect is moreover confirmed by direct simulations of oscillators coupled with a scale-free interaction network (Motter *et al.*, 2005a; Motter *et al.*, 2005b).

The optimal value of $\beta = 1$ has a very intuitive explanation as each unit i is connected to exactly k_i other oscillators, so that the sum over $j \in \mathcal{V}(i)$ contains k_i terms. When $\beta < 1$, the oscillators with larger degree are more strongly coupled than the ones with smaller degree. When $\beta > 1$, the opposite situation happens. In both situations, some oscillators will be more coupled than others and the most or least coupled ones will limit the synchronizability (Motter *et al.*, 2005c). This consideration can be simply generalized to weighted networks by showing that the synchronizability decreases when the nodes' strengths (see Chapter 1) become more heterogeneous (Zhou, Motter and Kurths, 2006). The effect of clustering and assortativity can be investigated by using analogous considerations (Motter *et al.*, 2005a; 2005c). In particular, while disassortativity enhances the synchronizability (Sorrentino, di Bernardo and Garofalo, 2007), the eigenratio λ_{max}/λ_2 generally increases if the clustering coefficient increases. In other words, local cohesiveness does not favor global synchronization, as also found in networks characterized by communities identified by cohesive groups of nodes (Donetti, Hurtado and Muñoz, 2005; Park *et al.*, 2006).

As we have seen in previous chapters, the centrality of nodes is not just characterized by their degree. An important indicator is the betweenness centrality that identifies nodes having a key role in keeping the network connected, thus allowing

the exchange of signals anywhere in the network. It is then natural to imagine that high betweenness nodes are the hot spots that are difficult to synchronize as they bridge parts of the networks which are otherwise disconnected and thus not synchronized. More precisely, Nishikawa *et al.* (2003) have shown that the increase of $\lambda_{\max}/\lambda_2$ mirrors the one of the betweenness centrality (see also Hong *et al.* [2004]). In this context, Chavez *et al.* (2005) have pushed further the reasoning of Motter *et al.* (2005c) to achieve synchronizability, and proposed a rescaling of the couplings of the equations (7.3) that reads as

$$\frac{\mathrm{d}\phi_i}{\mathrm{d}t} = F(\phi_i) - \frac{\sigma}{\sum_{j\in\mathcal{V}(i)} b_{ij}^a} \sum_{j\in\mathcal{V}(i)} b_{ij}^a [H(\phi_i) - H(\phi_j)], \tag{7.16}$$

where a is a parameter and b_{ij} is the betweenness centrality of the edge (i, j).[4] The case $a = 0$ corresponds to the optimal synchronizability of Equation (7.12), since in this instance $b_{ij}^a = 1$ and $\sum_{j\in\mathcal{V}(i)} b_{ij}^a = k_i$, while positive values of a give larger coupling strengths to the edges with large centrality. These edges are indeed crucial in holding the network together and ensuring communication (see Chapters 6 and 11). Numerical computation of eigenratios for various scale-free networks, as well as direct simulations of oscillators coupled according to (7.16), show that synchronizability is increased with respect to the case (7.12) for a close to 1. In fact, the procedure (7.16) is more efficient than the uniformization by the degree (7.12) because it weighs the links according to the global structure of network, rather than to local information.

7.2.3 Degree-related asymmetry

The couplings considered in the previous subsection are not symmetric, in contrast with the initial formulation (7.3). Asymmetric couplings between oscillators can in fact be studied with more generality. In most real-world networks indeed the interactions display some degree of asymmetry, due, for example, in social networks, to differences in age or social influence. In general, one can consider coupled oscillators evolving according to the set of equations (7.3) with an asymmetric coupling matrix $C_{ij} \neq C_{ji}$ (with obviously $C_{ij} = 0$ if i and j are not neighbors). The stability analysis of the synchronized state is then more involved, since the eigenvalues of $\mathbf{C}$ can be complex-valued. Let us simply mention that, if the eigenvalues $\lambda_j = \lambda_j^{\mathrm{r}} + i\lambda_j^{\mathrm{i}}$ ($i^2 = -1$) are ordered by increasing real parts λ_j^{r} ($0 = \lambda_1^{\mathrm{r}} \leq \lambda_2^{\mathrm{r}} \leq \cdots \leq \lambda_N^{\mathrm{r}} \equiv \lambda_{\max}^{\mathrm{r}}$), the best propensity for synchronization is

[4] As in the case of (7.12), the coupling is not symmetric but the coupling matrix is the product of the symmetric matrix with elements $b_{ij}^a L_{ij}$ and of the diagonal matrix $\mathrm{diag}\{1/\sum_j b_{1j}^a, \cdots, 1/\sum_j b_{Nj}^a\}$, so that its eigenspectrum is still real and non-negative.

https://doi.org/10.1017/CBO9780511791383.008 Published online by Cambridge University Press

obtained when the ratio of the largest to the smallest non-zero real parts, $\lambda^{\mathrm{r}}_{\max}/\lambda^{\mathrm{r}}_{2}$, and the quantity $M = \max_j\{|\lambda^i_j|\}$ are simultaneously made as small as possible (Hwang *et al.* [2005] and Boccaletti *et al.* [[2006]] for details).[5]

It is of course possible to study arbitrarily complicated forms for the coupling between oscillators. In the context of networks, a natural classification of nodes is given by their degree. An interesting example of asymmetric couplings consists therefore in an asymmetry depending on the nodes' degrees (Hwang *et al.*, 2005). In other words, the value of the coupling C_{ij} depends on the relative values of the degrees of the nodes i and j. In particular, one can compare the two following opposite situations. In the first situation, the couplings are such that $C_{ij} > C_{ji}$ for $k_i < k_j$. The influence of j on i is then larger than the influence of i on j, if j has a larger degree than i. The large degree nodes are thus "driving" the nodes with smaller degree. In the second situation, the asymmetry is reversed ($C_{ij} < C_{ji}$ for $k_i < k_j$), and a node with small degree will have a stronger influence on a neighbor with larger degree. In each case, the most extreme asymmetry is obtained when, for each link (i, j), one of the couplings C_{ij} or C_{ji} is equal to 0. A parameter can be introduced to tune the system from one extreme situation to the other. Hwang *et al.* (2005) then obtain that the propensity for synchronization is maximal when hubs completely drive the small nodes. This case is obtained by taking $C_{ji} = 0$ for $k_i < k_j$ (with on the other hand $C_{ij} \neq 0$), and corresponds in fact to strictly unidirectional couplings on each link (if j has an influence on i, it does not in return feel the influence of i). Such results can be understood intuitively by considering a star network consisting of a single hub connected to many nodes of degree 1. If the coupling is directed from the hub to the other nodes, synchronization will clearly be much easier than in the opposite case, in which the hub would receive uncorrelated inputs from the other nodes. Interestingly, this result is robust and remains valid even if the interaction network does not display strong degree fluctuations, for example in an Erdős–Rényi network.

Investigation of the effect of mixing patterns and degree correlations moreover leads to the conclusion that synchronizability is enhanced in *disassortative* scale-free networks when smaller nodes drive larger degree ones, while the better propensity for synchronization when the hubs are driving the small nodes is slightly improved in assortative networks (Sorrentino *et al.*, 2006). Synchronizability is therefore favored if hubs are strongly interconnected and drive the nodes with smaller degrees. In other words, a rich-club (Chapter 1) of large degree nodes will lead to a good synchronizability. Zhou and Kurths (2006) confirm this picture by showing that, even when the system is not fully synchronized, it displays a

[5] See also Nishikawa and Motter (2006a; 2006b) for the extension of the master stability function framework to directed, *weighted*, and *non-diagonizable* coupling matrices.

hierarchical synchronization in which the hubs are synchronized more closely and form the dynamical core of the network.

7.3 Non-linear coupling: firing and pulse

Let us now turn to some concrete examples of coupled oscillators and to their synchronization properties. In many biological systems the interaction between oscillators is not smooth but rather episodic and pulse-like. For example, neurons communicate by firing sudden impulses. Neurosciences are indeed particularly concerned with the understanding of collective dynamical phenomena such as the propagation of such coherent sensory signals through networks (Maass and Bishop, 1998; Koch, 1999). More generally, synchronization and rhythmic processes play an important role in physiology (Glass, 2001).

To shed light on how the interaction topology affects the collective behavior of coupled neurons, Lago-Fernández *et al.* (2000) have considered a system of non-identical neurons, each described by a set of coupled differential equations for the evolution of local currents and potentials. In this model, interaction between coupled neurons occurs through pulses, and various coupling topologies can be compared. On the one hand, regular topologies (grids) give rise to coherent oscillations but with a slow time scale for the system response and a relatively long transient. Completely random topologies on the other hand ensure a fast response of the system to external stimulation, but no coherent oscillations are observed. Interestingly, the Watts–Strogatz topology, with small distances between units and large clustering coefficient, displays both a fast system response and coherent global oscillations.

Such analysis can be extended to simpler and more general models of pulse driven oscillators. In particular, the integrate-and-fire model for synchronous firing of biological oscillators is based on Peskin's model (Peskin, 1975) of the cardiac pacemaker. This model describes a population of identical oscillators which communicate through sudden impulses. The firing of one oscillator is transmitted to its neighbors, possibly bringing them to the firing threshold. For simplicity, each oscillator is described by a phase $\theta_i(t) \in [0, 2\pi]$ which increases linearly in time. The evolution of the dynamical variable $\phi_i = \theta_i/2\pi$ is thus governed by the equation

$$\frac{\mathrm{d}\phi_i}{\mathrm{d}t} = 1, \tag{7.17}$$

until it reaches $\phi_i(t_i) = 1$. The oscillator's phase is then reset to 0 while it "fires" a signal to its neighbors $j \in \mathcal{V}(i)$, whose internal variables undergo a phase jump whose amplitude depends on their states. The global update rules when ϕ_i reaches 1 are thus given by

https://doi.org/10.1017/CBO9780511791383.008 Published online by Cambridge University Press

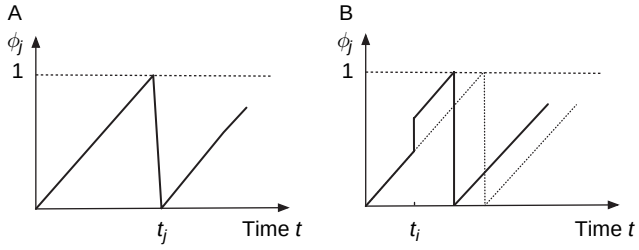

Fig. 7.4. A, Unperturbed evolution of a firing oscillator j according to (7.17) and (7.18). B, Evolution of ϕ_j when a neighbor i of j fires at t_i.

$$\phi_i(t_i) = 1 \Rightarrow \begin{cases} \phi_i(t_i^+) = 0 \\ \phi_j(t_i^+) = \phi_j(t_i) + \Delta\left[\phi_j(t_i)\right] \end{cases} \tag{7.18}$$

for all neighboring sites $j \in \mathcal{V}(i)$ of i, as illustrated in Figure 7.4. Here the function Δ, called the phase response curve, governs the interaction, and t_i^+ represents the time immediately following the firing impulse of node i. It is also possible to introduce a delay between the firing of the node i and the update of its neighbors. In this case we can consider that the firing signal takes a time τ to go from one oscillator to the other, yielding the update rule $\phi_j((t_i+\tau)^+) = \phi_j(t_i+\tau)+\Delta\left[\phi_j(t_i+\tau)\right]$. An interesting feature of the firing dynamics is the possibility of generating avalanches because if $\phi_j((t_i+\tau)^+)$ is larger than 1, the unit j fires in its turn and so on, triggering in some cases a chain reaction of firing events.

A generalization of the integrate-and-fire model (Mirollo and Strogatz, 1990) describes many different models of interacting threshold elements (Timme, Wolf and Geisel, 2002). In this generalization each oscillator i is characterized by a state variable function of the phase $x_i = U(\phi_i)$, which is assumed to increase monotonically toward the threshold 1. When x_i reaches the threshold, the oscillator fires and its state variable is set back to zero. The function $U(\phi)$ is assumed to be monotonic increasing ($\partial_\phi U > 0$), concave ($\partial_\phi^2 U < 0$), with $U(0) = 0$ and $U(1) = 1$. When the oscillator at node i fires, its neighbors $j \in \mathcal{V}(i)$ are updated according to the following rule

$$x_i(t_i) = 1 \Rightarrow x_j(t_i^+) = \min(1, x_j(t_i) + \varepsilon_{ji}), \tag{7.19}$$

where ε_{ji} gives the coupling strength between i and j. The interaction is excitatory if ε_{ji} is positive, and inhibitory if $\varepsilon_{ji} < 0$. In terms of the phase variable (see also Figure 7.5), the "pulse-coupled" model is therefore described by the set of equations

$$\phi_i(t_i) = 1 \Rightarrow \begin{cases} \phi_i(t_i^+) = 0 \\ \phi_j(t_i^+) = \min\{U^{-1}(U(\phi_j(t_i)) + \varepsilon_{ji}), 1\}. \end{cases} \tag{7.20}$$

https://doi.org/10.1017/CBO9780511791383.008 Published online by Cambridge University Press

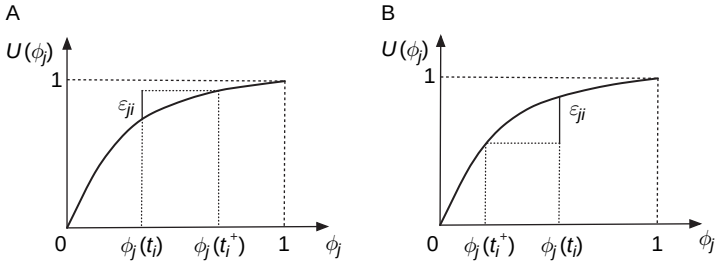

Fig. 7.5. Phase dynamics of oscillator j in response to the firing of a neighbor i of j at time t_i, according to (7.20), in the case of (A) an excitatory spike $\varepsilon_{ji} > 0$ and (B) an inhibitory spike $\varepsilon_{ji} < 0$.

In the case of zero delay ($\tau = 0$), Mirollo and Strogatz (1990) have shown that for arbitrary initial conditions a system of fully connected oscillators reaches a synchronized state in which all the oscillators are firing synchronously. The introduction of a positive delay $\tau > 0$ introduces a number of attractors increasing exponentially with the network size. Most of these attractors are periodic orbits that exhibit several groups of synchronized clusters of oscillators which fire and receive pulses alternatively. The above results refer to an operative and quantitative definition of the level of synchronization of the N interacting units expressed by the quantity

$$S = \frac{1}{N} \sum_{i=1}^{N} \left[1 - \phi_i(t_j^+) \right], \tag{7.21}$$

measured at each firing event of a reference unit j (the choice of the reference unit being arbitrary). This function approaches 1 when the system is completely synchronized. The *synchronization time* t_s can be defined as the time needed for S to reach 1, starting from random phases ϕ_i (Guardiola *et al.*, 2000), as shown in Figure 7.6. Interestingly, oscillators located on the nodes of regular lattices reach synchronization in a shorter time than in the case in which they are coupled through a random network with similar average degree. Further investigation shows that small-world topologies such as those induced by the Watts–Strogatz construction yield intermediate results. More precisely, the synchronization time is an increasing function of the rewiring parameter of the Watts–Strogatz model.

Like what is observed in the synchronizability of networks (see Section 7.2.2), the decrease in synchronizability as the network disorder increases is due to the variations in the number of neighbors and the ensuing fluctuations in the amplitude of the signals received by each unit. The role of degree fluctuations is clearly illustrated (Guardiola *et al.*, 2000) by using, for each oscillator i of degree k_i, a rescaled

https://doi.org/10.1017/CBO9780511791383.008 Published online by Cambridge University Press

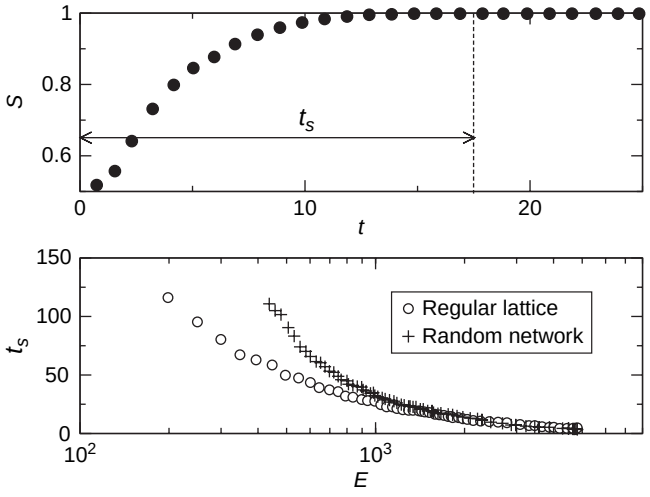

Fig. 7.6. Top: Evolution of the synchronization parameter given by Equation (7.21), and definition of the synchronization time t_s as the time needed to reach $S = 1$. In this case a population of 300 oscillators with random initial conditions is simulated. Bottom: Synchronization time t_s as a function of the number of edges E with a fixed number of oscillators $N = 100$ and interaction strength $\varepsilon = 0.01$ for the regular lattice and the Erdős–Rényi random graph. The regular lattice always performs better than the random graph although the difference quickly vanishes as E increases, i.e. as the network becomes more globally coupled. Data from Guardiola *et al.* (2000).

phase response $\Delta(\phi_i) \to \Delta(\phi_i)\langle k\rangle/k_i$ when a neighbor of i fires. This modification, in the same spirit as Equation (7.12) in Section 7.2.2, has the effect of making the couplings uniform and improving the synchronizability of networks. Some other results generally valid for arbitrary topologies can be obtained by studying particular coupling functions. For instance, it turns out that the stability of the synchronized state is ensured for inhibitory couplings ($\varepsilon_{ij} < 0$), whatever the network structure (Timme *et al.*, 2002). For arbitrary couplings on the other hand, firing times can be highly irregular (Brunel and Hakim, 1999; van Vreeswijk and Sompolinsky, 1996), and a coexistence of both regular and irregular dynamics may also be observed (Timme *et al.*, 2002). Finally, large heterogeneities in the coupling values tend to disrupt the synchronous state, which is replaced by aperiodic, asynchronous patterns (Denker *et al.*, 2004).

7.4 Non-identical oscillators: the Kuramoto model

Real coupled oscillators are rarely identical. In this spirit, a widely studied paradigm is defined by the Kuramoto model, which considers an ensemble of N

https://doi.org/10.1017/CBO9780511791383.008 Published online by Cambridge University Press

planar rotors, each one characterized by an angular phase ϕ_i and a natural frequency ω_i ($i = 1, \ldots, N$) (Kuramoto, 1984). These oscillators are coupled with a strength K, and their phases evolve according to the set of non-linearly coupled equations

$$\frac{\mathrm{d}\phi_i}{\mathrm{d}t} = \omega_i + K \sum_{j \in \mathcal{V}(i)} \sin(\phi_i - \phi_j), \tag{7.22}$$

where $\mathcal{V}(i)$ is the set of neighbors of i (see Acebrón *et al.* [2005] for a recent review). The natural frequencies and the initial values of the phases are generally assigned randomly from an a priori given distribution. For the sake of simplicity, the frequency distributions generally considered are unimodal and symmetric around a mean value Ω. The level of synchronization achieved by the N coupled oscillators is quantified by the complex-valued order parameter

$$r(t)\mathrm{e}^{\mathrm{i}\psi(t)} = \frac{1}{N} \sum_{j=1}^{N} \mathrm{e}^{\mathrm{i}\phi_j(t)}, \tag{7.23}$$

which can be seen as measuring the collective movement produced by the group of N oscillators in the complex plane. As shown schematically in Figure 7.7, each oscillator phase ϕ_j can be represented as a point moving around the circle of unit radius in the complex plane. Equation (7.23) then simply gives the position of the center of mass of these N points. The radius $r(t)$ measures the coherence, while the phase $\psi(t)$ is the average phase of the rotors. If the oscillators are not synchronized, with scattered phases, $r(t) \to 0$ in the so-called thermodynamic limit with $N \to \infty$. In contrast, a non-zero value of r denotes the emergence of a

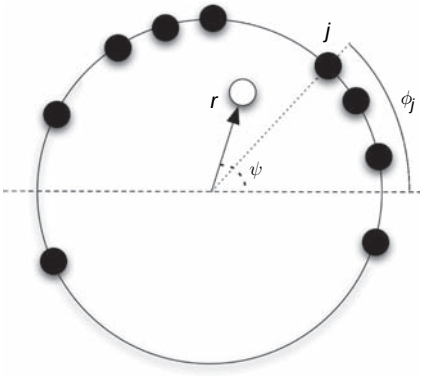

Fig. 7.7. Schematic presentation of the Kuramoto model: the phases ϕ_j correspond to points moving around the circle of unit radius in the complex plane. The center of mass of these points defines the order parameter (7.23), with radius r and phase ψ.

https://doi.org/10.1017/CBO9780511791383.008 Published online by Cambridge University Press

state in which a finite fraction of oscillators are synchronized. A value of r close to 1 corresponds to a collective movement of all the oscillators that have almost identical phases.

7.4.1 The mean-field Kuramoto model

A commonly studied version of the Kuramoto model considers a fully connected interaction network in which all the oscillators are coupled with the same strength $K = K^0/N$, with finite K^0 in order to ensure a regular limit $N \to \infty$ (Kuramoto, 1984). Effectively, each oscillator is affected by a non-linear coupling that is the average of the coupling with all other units, therefore defining a mean-field version of the model. The evolution equations (7.22) can be rewritten by introducing the order parameter (7.23). Multiplying both sides of (7.23) by $e^{-i\phi_\ell}$ and taking the imaginary part yields

$$r \sin(\psi - \phi_\ell) = \frac{1}{N} \sum_{j=1}^{N} \sin(\phi_j - \phi_\ell), \tag{7.24}$$

which allows Equation (7.22) to be written in the form

$$\frac{d\phi_\ell}{dt} = \omega_\ell + K^0 r \sin(\phi_\ell - \psi). \tag{7.25}$$

This rewriting of the oscillators equations highlights the mean-field character of the model, in which the interaction term is expressed as a coupling with the mean phase ψ, with intensity proportional to the coherence r (Strogatz, 2000b). The presence of a positive feedback mechanism is then clear: as more rotors become coherent, the effective coupling strength $K^0 r$ increases, which pushes still other rotors to join the coherent group. This mechanism arises in fact only if the coupling K increases above a critical value K_c. For $K^0 < K_c$, phases become uniformly distributed and $r(t)$ decays to 0 (or to fluctuating values of order $\mathcal{O}(N^{-1/2})$ at finite population size). When K^0 is increased above the critical value K_c, some elements tend to lock their phases and r becomes finite. Closer examination shows that the population of rotors is then divided into two groups: a certain number of oscillators oscillate at the common frequency Ω, while others (which have natural frequencies farther from the average) keep drifting apart. In this partially synchronized state, the group of synchronized nodes is composed by an increasing number of oscillators as K^0 grows, and r increases as schematically shown in Figure 7.8 (Strogatz, 2000b). More precisely, the transition between incoherent and coherent

https://doi.org/10.1017/CBO9780511791383.008 Published online by Cambridge University Press

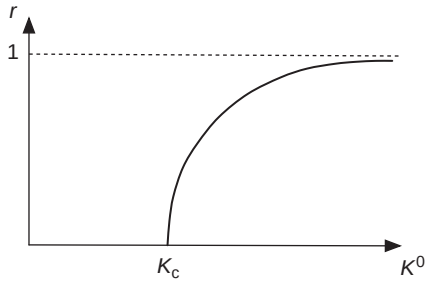

Fig. 7.8. Schematic mean-field result for the Kuramoto model. Below the critical coupling K_c there is no synchronization ($r = 0$). Above the threshold a finite fraction of the nodes are synchronized.

global dynamics is continuous: the order parameter behaves in the double limit of large sizes (thermodynamic limit $N \to \infty$) and times ($t \to \infty$) as

$$r = \begin{cases} 0 & K^0 < K_c \\ (K^0 - K_c)^\beta & K^0 \geq K_c \end{cases}, \tag{7.26}$$

where the precise value of K_c depends on the distribution of natural frequencies ω_i, and $\beta = 1/2$.

7.4.2 The Kuramoto model on complex networks

Strogatz and Mirollo (1988) have shown that the probability of phase-locking for Kuramoto oscillators located at the vertices of regular lattices vanishes as the number N of oscillators diverges. On the other hand, numerical simulations (Watts, 1999) have pointed out the existence of synchronized states when a small amount of disorder is introduced into the lattice through shortcuts, as in the small-world model network construction (Watts and Strogatz, 1998). By performing a detailed numerical investigation, Hong, Choi and Kim (2002a) have shown that the order parameter r, averaged over time and realizations of the intrinsic frequencies, obeys the finite-size scaling form

$$r(N, K) = N^{-\beta/\nu} F\left[(K - K_c)N^{1/\nu}\right], \tag{7.27}$$

where F is a scaling function and the exponent ν describes the divergence of the typical correlation size $(K - K_c)^{-\nu}$. The form (7.27) implies that at $K = K_c$, the quantity $rN^{\beta/\nu}$ does not depend on the system size N. This method allows numerical determination of K_c as well as β and ν. For any finite rewiring probability p in the Watts–Strogatz model, a finite K_c is obtained, and the exponents β and ν are compatible with the mean-field values $\beta \approx 0.5$ and $\nu \approx 2.0$, valid for the fully connected graph (Hong, Choi and Kim, 2002a).

https://doi.org/10.1017/CBO9780511791383.008 Published online by Cambridge University Press

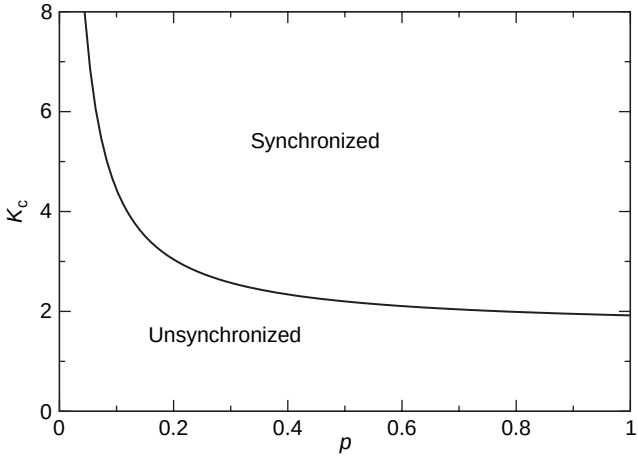

Fig. 7.9. Critical coupling K_c versus p for a small-world network of Kuramoto oscillators. Above the curve, the system is synchronized while below it does not show any extensive synchronization. Adapted from Hong, Choi and Kim (2002a).

As $p \to 0$, K_c diverges, as shown in Figure 7.9, in agreement with the results of Strogatz and Mirollo (1988). Moreover, the time needed to achieve synchronization decreases significantly when p increases. This global behavior is reminiscent of the case of the equilibrium Ising model evolving on small-world networks for which, as explained in Chapter 5, a phase transition of mean-field character appears at finite temperature as soon as p is finite.

Similar to other dynamical processes, the synchronization of Kuramoto oscillators may also be modified by large degree fluctuations in the coupling network. In order to analytically study the model in the case of oscillators with varying degree, it is possible to use an equivalence assumption for oscillators within the same degree class analogous to those used in other chapters of this book. By using this approximation, Ichinomiya (2004) finds that the critical coupling for uncorrelated random networks with arbitrary degree distribution is given by the expression

$$K_c = c\frac{\langle k \rangle}{\langle k^2 \rangle}, \tag{7.28}$$

where the constant c depends on the distribution of the individual frequencies ω (see also Restrepo, Ott and Hunt [2005a; 2005b]). The quantity $\kappa = \langle k^2 \rangle / \langle k \rangle$, which determines the heterogeneity level of the degree distribution, turns out once again to be the relevant parameter as for other processes such as equilibrium phase transitions (Chapter 5), percolation (resilience) phenomena (Chapter 6) or epidemic spread (Chapter 9). If the degree fluctuations are bounded, $\langle k^2 \rangle$ is finite as the size of the network approaches infinity, and K_c is finite. In the case of a heavy-tailed

degree distribution with a diverging second moment, on the other hand, the synchronization threshold goes towards zero in the limit of infinite size network. Hubs drive the dynamics and lead to synchronization for any finite coupling between nodes, just as, in the case of Ising spins, the hubs polarize the network and lead to a ferromagnetic state at any finite temperature (see Chapter 5). The role of the hubs is highlighted by the calculation of the average time $\langle\tau\rangle$ for a node to resynchronize after a perturbation, as a function of its degree. Moreno and Pacheco (2004) obtain numerically the behavior $\langle\tau\rangle \sim k^{-\mu}$ with μ close to 1: the larger the degree of a node, the more stable its synchronized behavior. Let us finally note that the mean-field approach also allows one to compute the critical behavior of the order parameter (Lee, 2005). For finite K_c, one obtains

$$r \sim \Delta^{\beta}, \tag{7.29}$$

where $\Delta \equiv (K - K_c)/K_c$ and, for a scale-free network with degree distribution $P(k) \sim k^{-\gamma}$, the exponent takes the value $\beta = 1/2$ if $\gamma > 5$ and $\beta = 1/(\gamma - 3)$ if $5 \geq \gamma > 3$.

Since the analytical results rely on a certain number of assumptions and on the degree classes equivalence approximation, it is worth mentioning that extensive numerical simulations have been performed for the evolution of Kuramoto oscillators on complex networks. An interesting result is reported by Moreno and Pacheco (2004) and Moreno, Vazquez-Prada and Pacheco (2004c) who find a non-zero threshold K_c for the onset of synchronization of oscillators interacting on a Barabási–Albert network. Such a discrepancy with the mean-field results could be due either to the inadequacy of the mean-field approximation, or to the fact that $\langle k^2\rangle$ diverges very slowly – logarithmically – with the network size in Barabási–Albert networks, possibly leading to an apparent finite value of K_c even at very large network sizes.

7.5 Synchronization paths in complex networks

The Kuramoto model of coupled oscillators described in the previous section represents a very interesting framework to study the effect of network topology on the synchronization mechanisms. The study of the order parameter r defined in (7.23) can be enriched by the definition of the link order parameter (Gómez-Gardeñes, Moreno and Arenas, 2007b)

$$r_{\text{link}} \equiv \frac{1}{2E} \sum_{j} \sum_{\ell \in \mathcal{V}(j)} \lim_{\Delta t \to \infty} \frac{1}{\Delta t} \int_{\tau}^{\tau + \Delta t} e^{i[\phi_j(t) - \phi_\ell(t)]}, \tag{7.30}$$

https://doi.org/10.1017/CBO9780511791383.008 Published online by Cambridge University Press

where E is the total number of links in the network and τ is a time large enough to let the system relax from its initial conditions. The quantity r_{link} quantifies the fraction of links that are synchronized in the network, and therefore gives more detailed information than r. In a hypothetical situation in which nodes would be synchronized by pairs for example, r, as the sum of $N/2$ random phases, could be very small while r_{link} would take a non-zero value. Even more insights are obtained from the full matrix

$$D_{j\ell} \equiv x_{j\ell} \left| \lim_{\Delta t \to \infty} \frac{1}{\Delta t} \int_{\tau}^{\tau+\Delta t} e^{i[\phi_j(t)-\phi_\ell(t)]} \right|, \tag{7.31}$$

where $x_{j\ell}$ is the adjacency matrix. A threshold T can then be used to distinguish pairs of synchronized nodes for $D_{j\ell} > T$ from unsynchronized neighbors for $D_{j\ell} < T$.

The combined study of r and r_{link} as a function of the coupling strength of Kuramoto oscillators located on the nodes of Erdős–Rényi and Barabási–Albert networks with same average degree reveals a very interesting picture (Gómez-Gardeñes, Moreno and Arenas, 2007b; 2007c). By varying the coupling strength it is first observed that the critical coupling is strongly decreased by the heterogeneity of the network. At large coupling however, the homogeneous topology leads to a stronger synchronization with larger r values. Strikingly, r_{link} takes non-zero values as soon as the coupling is non-zero, even in the non-synchronized phase with $r = 0$, illustrating the existence of local synchronization patterns even in the regime of global incoherence. The detailed study of the clusters of synchronized nodes, available through the measure of the matrix elements (7.31), shows that the largest cluster of synchronized oscillators contains almost half of the network nodes as the coupling approaches the critical value, and that many smaller clusters of synchronized nodes are present as well.

Figure 7.10 schematically displays the evolution of synchronized clusters as the coupling is increased. For homogeneous networks, a percolation type process is observed in which small synchronized clusters appear and coalesce at larger coupling strength in a sharp merging process towards the complete synchronization of the network. In contrast, the synchronization of a scale-free network is organized around its hubs, which first form a central synchronized core and then aggregate progressively the other small synchronized clusters as the coupling is strengthened. These results emphasize the role of the hubs in the emergence of cohesion in complex networks, as also noticed in other problems such as network resilience and rumor spreading (Chapters 6 and 10).

https://doi.org/10.1017/CBO9780511791383.008 Published online by Cambridge University Press

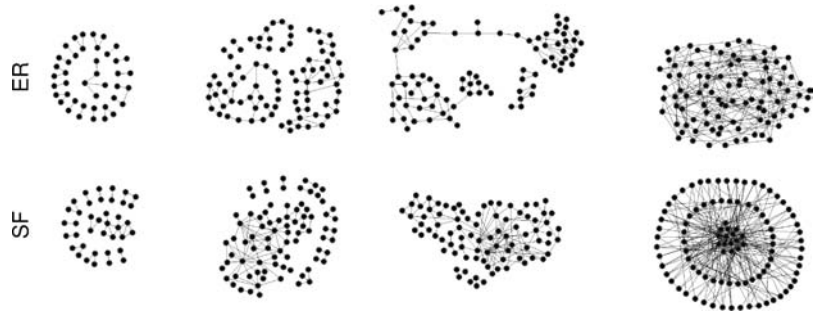

Fig. 7.10. Synchronized clusters for two different topologies: homogeneous and scale-free. Small networks of 100 nodes are displayed for the sake of visualization. From left to right, the coupling intensity is increasing. Depending on the topology, different routes to synchronization are observed. In the case of Erdős–Rényi networks (ER), a percolation-like mechanism occurs, while for scale-free networks (SF), hubs are aggregating more and more synchronized nodes. Figure courtesy of Y. Moreno, adapted from Gómez-Gardeñes, Moreno and Arenas (2007b).

7.6 Synchronization phenomena as a topology probing tool

The various studies on the synchronizability of complex networks have shed light on the basic mechanisms through which the topological features affect the capacity of oscillators to reach a synchronized state. Networks' topological characteristics are, however, not limited to their homogeneous or heterogeneous character. For instance, Park *et al.* (2006) have shown how community structures strongly influence the synchronizability of networks. Analogously, Oh *et al.* (2005) and Timme (2006) show for Kuramoto oscillators that rather different synchronization properties are obtained for different kinds of modular structure, even with similar degree distributions.

In other words, the detailed structure and connectivity pattern of networks are extremely relevant in determining the synchronizability of systems. This evidence suggests an inverse approach to the problem in which the synchronization behavior is used as a probe for the understanding of the community and modular structure of networks. The community detection problem in large-scale networks is in fact a very difficult task, which has generated a large body of work. Intuitively, and using a simple topological approach, a community in the network can be defined as a densely interconnected subgraph whose number of connections to nodes outside the subgraph is much smaller than the number of connections within the subgraph. The precise mathematical definition of a community is more elusive, and various formal or operative definitions have been put forward in the literature. At the same time, various algorithms have been proposed in order to

find partitions of a network's subgraphs in order to capture the presence of communities according to various rigorous and less rigorous definitions (for recent reviews, see Newman [2004] and Danon *et al.* [2005]). In this context, the study of synchronization behavior and the eigenvalue spectra of networks represents an interesting alternative. In particular, it turns out that, during the *transient towards synchronization*, modules synchronize at different times and in a hierarchical way. In this way the approach to the synchronized regime is able to progressively identify the basic modules and community of the network. The study of the synchronization properties can then be approached by looking at the dynamical behavior of the system or by the analysis of the eigenvalue spectrum of the network (Donetti and Muñoz, 2004; Capocci *et al.*, 2005; Arenas, Díaz-Guilera and Pérez-Vicente, 2006a; 2006b). In both approaches a wealth of information on the detailed structure of the network can be obtained by simply looking at the basic characterization of the dynamical properties of coupled oscillators.